ELSEVIER

Catalysis Today 48 (1999) 337–345

CATALYSIS TODAY

Kinetic experiments and modeling of a three-phase catalytic hydrogenation reaction in supercritical CO_2

L. Devetta[a,*], A. Giovanzana[a], P. Canu[a], A. Bertucco[a], B.J. Minder[b]

[a]*Istituto di Impianti Chimici, Università di Padova, Padova, Italy*
[b]*F. Hoffmann La-Roche AG, Basel, Switzerland*

Abstract

The three-phase catalytic hydrogenation of an unsaturated ketone using supercritical carbon dioxide as a solvent was studied in order to simulate the performance of a semi-industrial trickle-bed reactor. High pressure kinetic experiments were carried out in a modified internal recycle reactor of Berty type. An industrial Pd on alumina supported catalyst was used, in form of egg-shell pellets. Data were collected over the whole conversion range, allowing for a thorough inspection of the reaction rate composition dependencies. It is shown that supercritical CO_2 strongly increases the reaction rate. Experimental data sets were fit using both simple homogeneous power-law kinetics and complex heterogeneous Langmuir–Hinshelwood models: here, the estimation of liquid concentrations was performed through vapor–liquid equilibrium calculations based on an equation-of-state approach.

Keywords: Kinetic; Catalytic; Hydrogenation; CO_2

1. Introduction

Supercritical fluids (SCF) have unique properties which make them attractive as reaction solvents, as reviewed by Savage et al. [1]. Among others, advantages to conventional processes are: the enhanced solubility of gaseous reactants with respect to the liquid phase [2], the in situ catalyst reactivation with respect to carbonaceous byproducts; higher mass and heat transfer efficiencies [3]; consistent reduction of the reaction volume; environmental friendly properties of most frequently used supercritical solvents, e.g. H_2O and CO_2.

As summarized in a review by Mills et al. [4], many hydrogenations of interest to the fine chemicals and pharmaceuticals industries have already been studied extensively, mostly at low pressure in slurry reactors. On the other hand, there is little kinetic information published for reactions in supercritical solvents; on hydrogenation and de-hydrogenation heterogeneously catalyzed reactions only few works are reported [1].

The present work deals with a kinetic investigation of the high pressure hydrogenation reaction of organics on a supported metal catalyst, using supercritical CO_2 ($ScCO_2$) as a substitute solvent. Note that, as usual, with ''supercritical'' it is meant that the solvent itself is such at the operating conditions. However, the system contains also other components, so that, at the same conditions, there could be a coexistence of vapor and liquid phases.

The motivation of our work is to provide an accurate kinetic model for the scale-up of a pilot trickle-bed

*Corresponding author.

0920-5861/99/$ – see front matter
PII: S0920-5861(98)00390-3

reactor, as outlined by Devetta et al. [5]. To achieve this point, it is essential to develop tools suitable to represent correctly both phase equilibria and reaction rates; while equation-of-state based models sufficient to this scope are already available, and allow quantitative predictions of the multicomponent behavior from binary equilibrium data, the reaction kinetics must be determined experimentally. Extensive data will be reported and discussed. They will be correlated by kinetic models ranging from simple first order to detailed Langmuir–Hinshelwood (LHHW) expressions.

2. Experimental

2.1. Materials

The reaction considered is the two double bond hydrogenation of an unsaturated ketone of generic structure R_1–CH=C=CH–C(=O)–R_2 (identified in the following as component A). The desired product is the corresponding saturated ketone (referred to as component C). The feed mixtures (from Hoffmann-La Roche) include the main reactant (A) and three of its isomers (D): since isomerization reactions can occur in the on-line gas chromatographic column, A and D had to be considered as a unique pseudo-component, named AD. The partially hydrogenated isomers (one hydrogen bond) were named E, without further distinction.

On the base of previous assumptions, the reference reaction scheme is

$$\begin{aligned} AD + H_2 &\rightarrow E \\ E + H_2 &\rightarrow C \end{aligned} \quad (1)$$

Three organic feed mixtures, identified as a, b and c, have been used, in order to allow a more effective variation of the residence time, as discussed below. Their composition is reported in Table 1. CO_2 and H_2 feed flow rates were varied as well, as reported later on.

The reaction occurs on an industrial 0.5% Pd on alumina supported catalyst (Engelhard): egg-shell pellets of 3 mm nominal size were used to reduce internal mass-transfer limitations.

Table 1
Composition of three different organic feed mixtures used (weight fractions). Their use allowed more effective variation of residence time in the reactor, and thus of the conversion range investigated experimentally

Symbol	AD	E	C	Inerts
a	0.9602	0.0010	0.0000	0.0388
b	0.5360	0.3930	0.0350	0.0360
c	0.0912	0.3550	0.5170	0.0368

2.2. VLE calculations

When working with reactions in SCFs it is essential to be aware of the phase behavior exhibited by the reacting mixture, as pointed out by several authors [1,6]. Here, the equilibrium composition between existing phases has been evaluated through the Peng–Robinson equation of state (PR EOS). Binary interaction parameters were fitted on high pressure experimental VLE data, as reported by Bertucco et al. [7]. In that work, it was shown that the PR EOS provides an accurate correlation of experimental data, and could be reliably used to describe the behavior of the high pressure multicomponent system studied in this work. Particularly, phase-envelope diagrams (i.e. P versus T at a fixed composition) were generated to investigate the phase behavior of the mixture at the reaction conditions [5]. It was concluded that, owing to technical and economical reasons, the reaction must be carried out in the presence of both liquid and vapor phases. Therefore, three phases are involved in this reaction: the solid catalyst, a vapor and a liquid phase. The latter is where the reaction takes place and contains the organics, part of the CO_2 and dissolved hydrogen.

Note that, in our case, the main advantage of using $ScCO_2$ as a solvent is the enhanced hydrogen solubility in the liquid phase [1]. In this respect, quantitative informations on liquid phase composition obtained by applying the PR EOS model are plotted in Fig. 1. Here, the calculated solubility of hydrogen in the liquid phase compositions is reported as a function of CO_2-to-organic feed ratio at a temperature of 373 K and pressures ranging from 5 to 25 MPa.

A maximum is observed around 50 wt% CO_2, i.e. when the same amount of solvent and organics are fed to the reactor. Beyond that value, the curve decreases

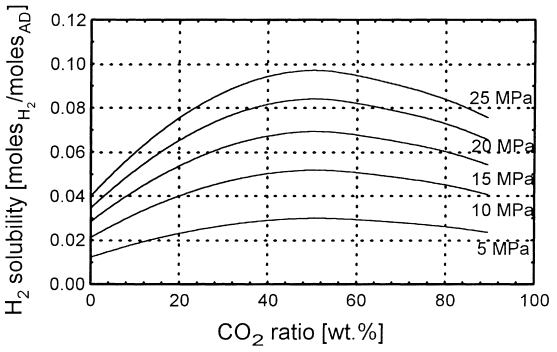

Fig. 1. Calculated liquid hydrogen solubility at different CO_2-to-organic feed ratios. Results are plotted as moles of gas dissolved per mole of reactant AD at T=373 K.

since higher dilution is not accomplished by further improvement of solubility. It is clear that the hydrogen solubility may be enhanced by the supercritical solvent up to three-fold. A similar behavior is observed at temperatures other than 373 K as well.

2.3. Experimental set-up and procedures

The laboratory apparatus is a differential internal-recycle reactor [8,9] of about 0.3 l total volume, modified for high temperature and high pressure reactions [10,11]. A detailed description is reported in [7].

Recycle reactors operating at very high internal-recycle ratios approximate quite well differential conditions on the catalyst bed [9], even though inlet and outlet streams have significantly different composition. Moreover, they can be regarded to as a perfectly mixed reactor (CSTR): tracer experiments have confirmed that our reactor closely matches ideal mixing conditions. Therefore, reliable composition measurements of both inlet and outlet streams allow direct and accurate determination of reaction rate data.

Reactor temperature and pressure, and feed flow rates (liquid organic mixture, carbon dioxide and hydrogen) were continuously monitored and controlled by an Eurotherm TC S1000 process control unit. Start-up and shut-down procedures were completely automated, allowing for a high reproducibility level.

The product stream was flashed to ambient pressure in the product tank, where a cyclone-type separator recovers completely the organics and removes CO_2 and the unreacted hydrogen. The product analysis is performed on-line by a Siemens Sichromat RCG 202 gas chromatograph with FID. According to the CSTR behavior of recycle reactors, GC product measurements at normal pressure are used to estimate the reactor liquid phase composition [7], being CO_2 and H_2 determined from flow measurements and stoichiometry, respectively.

A number of improvements were carried out by modifying the experimental set-up with respect to our previous study [7]. The mixing turbine efficiency was enhanced by means of a more powerful engine, which allowed higher rotating speeds. A pre-heater was added in the feed line to minimize risks of temperature gradients through the catalyst bed. More accurate CO_2 and H_2 flowmeters have been installed.

The most relevant modification was the lining of the internal reactor wall. During the preliminary experimental runs, catalytic activity of the reactor surface was observed. Comparing experiments with and without catalyst, up to 43% of total yield was attributed to the reactor surface. Indeed, Pd adsorption in the steel surfaces gives them a catalytic activity which slowly decays, making impossible to evaluate the contribution of the catalyst bed. This problem, common to most hydrogenation reactors, has been solved covering with a very thin layer of titanium nitrite (TN) the whole reactor internals. The extremely compact structure of TN prevents adsorption of palladium, being furthermore resistant to the particular process conditions: high pressure (up to 25 MPa), high temperature (up to 523 K), high stirring speed (3000 rpm) and supercritical CO_2, which is a very good solvent for most organic compounds.

To avoid further deposition of palladium on the lined surface, the reactor was washed with CO_2 after each data point determination and with vaporized ethanol after each catalyst batch. Reactor temperature and pressure set points were reached under pure CO_2 flow, either to minimize disturbances and to keep the catalyst clean. This avoided coke accumulation into the pores during the subcritical phase of reactor start-up, as discussed by Saim and Subramaniam [12]. Details on the experimental procedure are reported in our previous work [7].

3. Results and discussion

Preliminary experiments were carried out to optimize the apparatus configuration and operating conditions. Experimental reproducibility was checked first, with good results. Several GC measurements were taken for each set of operating conditions, either to assess the steady state condition and to provide a representative sample of data.

The reactor hydrodynamic was studied to verify complete catalyst wetting and a uniform flow through the bed. Several internals (structured packings, size reducers) and bed positions were tested, leading to a final internal reactor configuration that allows the catalyst wetting efficiency to be close to 1. This conclusion is supported also by the high interaction regime (HIR, as defined for trickle-bed reactors) occurring in the catalyst bed at the conditions considered.

To check the presence of external mass-transfer limitations, measurements of the product conversion vs. the stirring speed at different catalyst amounts were performed. As expected, with larger catalyst mass, external mass transfer becomes more critical, and a higher stirring speed is required; however, after a threshold value, the kinetic becomes independent of agitation, as shown in Fig. 2. We also checked the absence of pore diffusion limitations for our egg-shell type catalyst: from experiments performed with the same amount of entire and fragmented catalyst pellets, it resulted that internal mass-transfer limitations can be neglected.

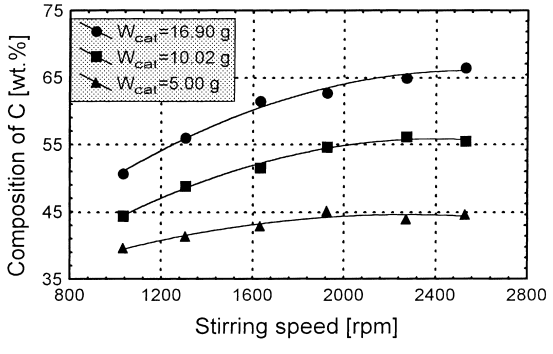

Fig. 2. External mass-transfer check. Three catalyst amounts were investigated at T=573 K, P=20 MPa, $F_{AD} = F_{CO_2} = 10\,g/min$, $F_{H_2} = 4\,NL/min$.

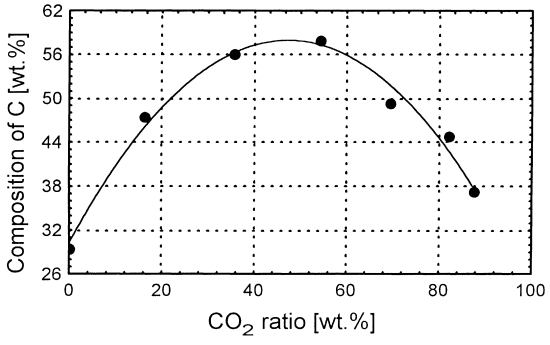

Fig. 3. CO_2 effect on reaction yield at T=573 K, P=20 MPa, $F_{AD} = 10\,g/min$, $F_{H_2} = 4\,NL/min$. Catalyst amount was 15 g.

Influence of the CO_2 on the reaction rate was verified, as shown in Fig. 3. The maximum reaction yield was obtained with 50 wt% CO_2 on total feed. Note that this is in agreement with the amount of hydrogen in the liquid phase, as depicted by Fig. 1.

Furthermore, a linear increase of the reaction kinetics with total pressure was detected up to nearly 20 MPa. It is not worthwhile to overcome that value, since the yield increases more slowly and mechanical stress becomes relevant. The maximum reactor temperature allowed by our experimental apparatus was 520 K.

Finally, it should be discussed if CO_2 can play the role of a reactive solvent. In our system, two reactions might occur: the CO_2 hydrogenation to formic acid, and its reduction to CO and methanol. The former can be excluded due to absence of amines in the reacting system, as pointed out by Jessop et al. [13]. The latter is possible on Pd-supported catalysts: it is favored by high temperatures [14] and residence times. Anyway, it produces water, which was never found in our reactor effluent. Consequently, we can exclude that CO_2 is taking part in any reaction.

3.1. Kinetic measurements

Since the present study supports the development of an industrial scale, catalytic, trickle-bed reactor [5], where the whole conversion is achieved, it was necessary to investigate a large conversion range. Hence, experimental conditions were chosen as displayed in Table 2. Note that CO_2 was always operated at 1/1 ratio to the organic feed and H_2 with 20% excess to the

Table 2
Experimental range of operating conditions for final kinetic investigations

Temperature (K)	Pressure (MPa)	$F_{organics}$ (g/min)	F_{CO_2} (g/min)	F_{H_2} (NL/min)	W_{cat} (g)
323–453	20	10–60	10–60	1.9–11.4	2–17

stoichiometric value. With the values adopted, the residence time was varied in the range between 0.03 and 2.05 min. Composition effects were studied by feeding partially reacted mixtures, attained by diluting product C with the reactant AD. In such respect, feed mixtures a, b, and c of Table 1 can be regarded as more and more converted mixtures, respectively.

Some insight of the actual kinetic mechanism and equations is provided by concentration vs. residence time and reaction rate vs. concentration plots.

Note that all concentration values are referred to the liquid phase, where the reaction takes place; they were estimated through high pressure VLE calculations as discussed in Section 2.2.

In Fig. 4 the concentrations of reactant AD, intermediate E and product C are plotted vs. residence time at 323 K. These results show an exponentially decreasing behavior toward zero for AD, as expected in an irreversible reaction. It can also be observed that the concentration of E has a flat maximum: this is consistent with E being an intermediate in a series reaction. As expected, product C concentration steadily increases with residence time. The same behavior has been evidenced at other temperatures investigated, as shown for AD in Fig. 5.

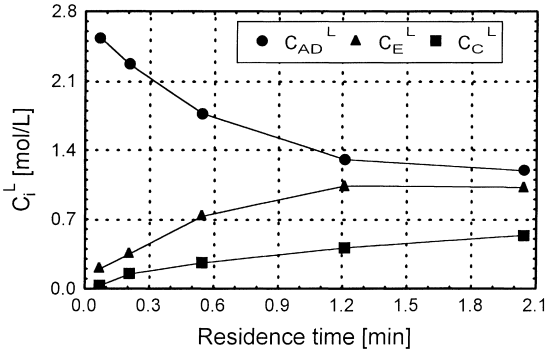

Fig. 4. Concentration profiles of organics as a function of residence time at T=323 K, P=20 MPa, $F_{AD} = F_{CO_2}$ = 10–50 g/min, F_{H_2} = 1.9–9.5 NL/min, W_{cat}=2–10 g. Feed was always of type a.

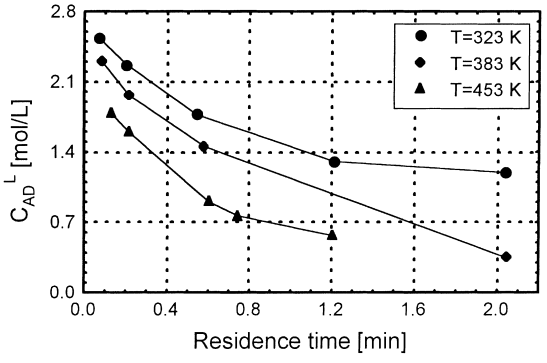

Fig. 5. Concentration profiles of organics as a function of residence time at T=323–383–453 K, P=20 MPa, $F_{AD}=F_{CO_2}$= 10–60 g/min, F_{H_2}=1.9–11.4 NL/min, W_{cat}=5–10 g. Feed was always of type a.

Results obtained with partially reacted feed mixtures always show almost zero reactant concentration: this can be explained by considering that the residence time was larger than required to reach total conversion. It turns out that a starvation regime arises in these cases: the consumption rate reflects the feed flow rate, independently of the concentration of reactants. Accordingly, the total residence time should be calculated by summing up the actual one and the one needed to get the feed conversion. In such a way the results would confirm the exponentially decreasing trend observed.

It is well known that the CSTR behavior of internal-recycle reactors provides kinetic data by simply applying the following mass balance:

$$r_j = \frac{LF}{W}\left(X_{j,\mathrm{i}} - X_{j,\mathrm{o}}\right)\frac{1}{PM_{j,\mathrm{i}}}, \qquad (2)$$

LF being the organic feed mass flow rate, W the mass of catalyst, X_j the weight fraction in the inlet (i) and outlet (o) organic streams and PM_j the molecular weight of component j. From Eq. (2) the production or consumption rate of component j, r_j, can be evaluated directly.

Fig. 6 shows the dependence of r_{AD} vs. hydrogen concentration. A positive partial reaction order is

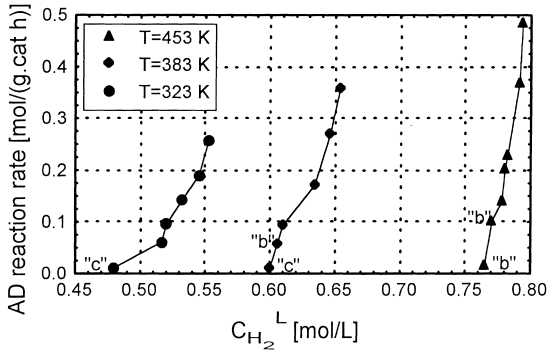

Fig. 6. Reaction rate of reactant AD as a function of hydrogen concentration in the liquid phase at T=323–383–453 K, P=20 MPa, $F_{AD}=F_{CO_2}$=10–60 g/min, F_{H_2}=1.9–11.4 NL/min, W_{cat}=2–17 g. Only feeds other than type a are labeled.

suggested for hydrogen. Note that the hydrogen solubility in the liquid phase increases with temperature at high pressure, as already noted for similar systems [15].

As far as the second reaction step is concerned, according to Fig. 7, the intermediate concentration (E) shows a maximum when plotted vs. the production rate of C. Such a behavior reflects the mechanism of a series reaction, where the product formation is slower than that of the intermediate.

3.2. Kinetic modeling

It is assumed that the vapor–liquid equilibrium is established in the system much faster than any reactive

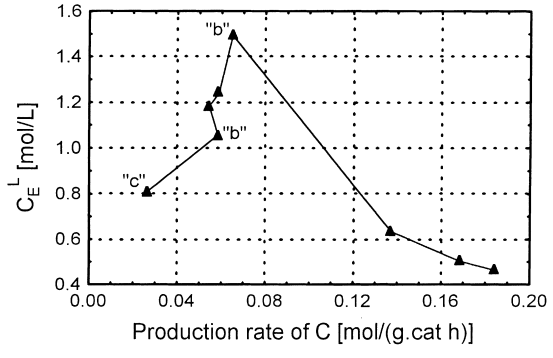

Fig. 7. Concentration of the intermediate as a function of production rate of C at T=453 K, P=20 MPa, $F_{AD}=F_{CO_2}$=10–40 g/min, F_{H_2}=1.9–7.6 NL/min, W_{cat}=5–17 g. Only feeds other than type a are labeled.

events. Such a hypothesis allows to decouple equilibrium and reaction dynamics. Moreover, complete chemical control can be assumed on the base of previous remarks about mass-transfer limitations.

The kinetic mechanism postulates that the reaction path follows the stoichiometry of Eq. (1). Single hydrogenations were split into elementary steps according to the classical adsorption-surface reaction-desorption scheme.

Several mechanisms, based on bimolecular surface reactions, were developed and tested: either two species adsorbed on the same type of active site, or one adsorbed molecule and one in the bulk (Eley–Rideal), or two adsorbed species on adjacent but different sites were considered.

Rate constants of elementary surface reactions are assumed only temperature dependent, according to the standard Arrhenius law: pressure dependency should not be significant in the experimental range examined, as already suggested [1]. Sometimes, temperature dependency of equilibrium adsorption rates have been introduced too, according to an exponential Van't Hoff expression.

A multivariable regression of experimental data was performed for any postulated mechanism, with liquid concentrations and temperatures as the independent variables and reaction rates as the dependent ones. A standard least-squares routine (Micromath Scientist) was used to estimate kinetic and adsorption parameters. The comparison among the models proposed was based on the estimated standard deviation of the model, σ, and *R-squared*. A result summary of the models considered is presented in Table 3, including parameter values and statistics.

As a first approach, we tried to develop models which consider the same adsorption mechanism for both steps, the only difference being in the elementary surface reaction. Unfortunately, this led to unsatisfactory results, as shown in Table 3 for models H-I-3 and H-II-3, for the first (AD→E) and second hydrogenation step (E→C), respectively. We concluded that different models had to be proposed for each step. In addition, it was attempted to verify whether CO_2 is adsorbed on active sites: however, models including this assumption resulted in worse agreement with experimental data, as seen for the model H-II-6 in Table 3.

Table 3
Model description and results for both reaction steps

Name	Model equation	Parameters	Statistics
H-I-3	$-r_{AD} = \frac{kK_{AD}C_{AD}K_{H_2}C_{H_2}}{\left(1 + K_{AD}C_{AD} + K_E C_E + K_C C_C + \sqrt{K_{H_2}C_{H_2}}\right)^3}$, $k=A\exp(E/T)$	A=229.6, E=1207.4, K_{AD}=0.5643, K_E=1.6157, K_C=1.0415, K_{H_2} = 4.6072	σ=0.0771, R^2=0.920
H-II-3	$r_C = \frac{kK_E C_E K_{H_2}C_{H_2}}{\left(1 + K_{AD}C_{AD} + K_E C_E + K_C C_C + \sqrt{K_{H_2}C_{H_2}}\right)^3}$, $k=A\exp(E/T)$	A=16.8, E=761.6, K_{AD}=0.5643, K_E=1.6157, K_C=1.0415, K_{H_2} = 4.6072	σ=0.0650, R^2=0.643
H-II-6	$r_C = \frac{kK_E C_E K_{H_2}C_{H_2}}{\left(1 + K_{CO_2}C_{CO_2} + K_E C_E + K_C C_C + K_{H_2}C_{H_2}\right)^3}$, $k=A\exp(E/T)$	A=56.0, E=1279.2, K_{CO_2} = 3909.9, K_E=3492.1, K_C=338.8, K_{H_2} = 174.7	σ=0.0184, R^2=0.967
P-I-1	$-r_{AD} = kC_{H_2}C_{AD}$, $k=A\exp(E/T)$	A=2.026, E=835.8	σ=0.0362, R^2=0.973
H-II-12	$r_C = \frac{kK_E C_E K_{H_2}C_{H_2}}{\left(1 + K_E C_E + K_C C_C + \sqrt{K_{H_2}C_{H_2}}\right)^3}$, $k=A\exp(E/T)$	A=391.7, E=1362.4, K_E=1.77, K_C=0.7269, K_{H_2} = 0.2021	σ=0.0167, R^2=0.968

Notation: H – heterogeneous, P – pseudo-homogeneous; I – first step, II – second step. Units for activation energy are kcal/mol.

According to our approach, we found that the first step is better described by a Langmuir–Hinshelwood mechanism, where the catalytic surface is supposed scarcely covered by both reactants, resulting in a pseudo-homogeneous-like correlation, first order in both the organic and gaseous reactant. This might explain the experimental evidence that the first hydrogenation step is extremely fast, without any quantitative adsorption. Similar models are indeed reported in the literature for hydrogenations on Pd-based catalysts [4]. The best kinetic equation is identified as P-I-1 in Table 3.

A parity plot of the first hydrogenation step is presented in Fig. 8(a). Most data fall in the range ±10%, but some experiments yielded unexpected results. The same outliers are unexplainable also when compared to the expected behavior of Figs. 5 and 6; therefore, they were eventually rejected in the parameter estimation procedure. This may be due to difference in the reactivity of components A and D; however, no analytical techniques were available to accurately quantify the isomers' content.

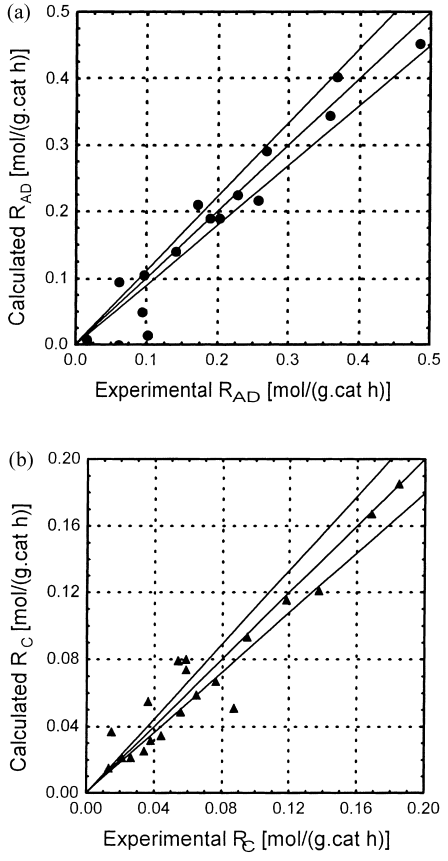

Fig. 8. Parity plots of reaction rates: first reaction step (a), and second reaction step (b). All experiments are displayed, including feeds of type a, b and c. The ±10% range is shown.

The second double bond hydrogenation is better fit by an Eley–Rideal mechanism. This model includes the dissociative, temperature-dependent adsorption of hydrogen and is indicated with H-II-12 in Table 3. The comparison between experimental and calculated results for the second reaction step is shown in Fig. 8(b). The ±10% range is reported as above. The same outliers are present here too.

Note that activation energy values of Table 3 are of the same order of magnitude as those reported in the literature for the hydrogenation on Pd catalysts [16,17].

Finally, it should be pointed out that also pure power-laws models, whose results are not reported here, are suitable for both steps, although they do not help to identify any actual mechanism of the reaction.

4. Conclusions

A high pressure experimental set-up for multiphase kinetic investigations was used. A Berty type internal-recycle reactor was modified and optimized in the internal fluid path, to study the three-phase hydrogenation of an unsaturated ketone with supercritical CO_2 as a solvent.

Catalyst wetting and absence of both internal and external mass-transfer limitations were checked, allowing accurate and reproducible kinetic data to be obtained. The catalytic activity of the internal reactor surface, due to adsorbed palladium fines, was strongly reduced by lining with titanium nitrite.

Experiments were carried out at 20 MPa and temperatures ranging from 323 to 453 K. Due to the large hydrogen content, the reaction was demonstrated to be a three-phase one at these conditions.

The results proved the positive effect of supercritical CO_2 on the reaction yield: optimal reaction conditions were identified at 1:1 CO_2 to liquid feed ratio, where product conversion doubles with respect to the absence of supercritical solvent.

Experimental data were fit in order to derive suitable kinetic equations. The first reaction step was well described by a pseudo-homogeneous model, first order in both reactants. A heterogeneous expression based on the Eley–Rideal mechanism was determined for the second step.

Acknowledgements

The authors are very grateful to Dr. Kurt Steiner of Hoffmann-La Roche for supporting this research project, and to Dr. Frank Lucien, University of South Wales (Aus), for the patience and help demonstrated during the experiments.

References

[1] P.E. Savage, S. Gopalan, T.I. Mizan, C.J. Martino, E.E. Brock, AIChE J. 41 (1995) 1723–1778.
[2] P.G. Jessop, T. Ikariya, R. Noyori, Science 269 (1995) 1065–1069.
[3] A.A. Clifford, in: Supercritical Fluids: Fundamentals for Applications, Series E: Appl. Sci., vol. 273, Kluwer Academic Publishers, Dordrecht, (1994) 449–480.
[4] P.L. Mills, P.A. Ramachandran, R.V. Chaudari, Rev. Chem. Eng. 8 (1992) Nos. 1–2.
[5] L. Devetta, P. Canu, A. Bertucco, K. Steiner, Chem. Eng. Sci. 52 (1997) 4163–4170.
[6] B. Subramaniam, M.A. McHugh, Reactions in supercritical fluids – A review, Ind. Eng. Chem. Process Des. Dev. 25 (1986) 1–12.
[7] A. Bertucco, P. Canu, L. Devetta, A.G. Zwahlen, Ind. Eng. Chem. Res. 36 (1997) 2626–2633.
[8] J.M. Berty, Catal. Rev.-Sci. Eng. 20(1) (1979) 75–96.
[9] J.M. Berty, Plant/Oper. Prog. 3 (1984) 163–168.
[10] A. Zwahlen, J. Agnew, in: Proceedings of the CHEMECA, Melbourne, Australia, vol. 1, 1987, pp. 50.1–50.7.
[11] A. Zwahlen, J. Agnew, Plant/Oper. Prog. 11 (1992) 166–168.
[12] S. Saim, B. Subramaniam, J. Catal. 131 (1991) 445.
[13] P.G. Jessop, T. Ikariya, R. Noyori, Nature 368 (1994) 231–233.
[14] P.G. Jessop, Personal communication, 1998.
[15] E. Brunner, J. Chem. Eng. Data 30 (1985) 269–273.
[16] R.S. Mann, A.M. Shah, Can. J. Chem. 50 (1972) 1793–1796.
[17] R. Van Eldik, T. Asano, W.J. Le Noble, Chem. Rev. 89 (1989) 549–688.